terminally differentiated cell types (**Fig. 4c**). We probed the epithelial permeability of the engrafts using tetramethylrhodamine isothiocyanate (TRITC)-conjugated dextran (TRITC-dextran). Blood TRITC concentrations in transplanted mice were comparable to those in control mice, indicating a maintenance of epithelial barrier function in these engrafts (**Fig. 4d**). Notably, transplantation was less successful with freshly isolated donor cells ($P < 0.05$, Mann-Whitney U test; **Supplementary Fig. 5**), suggesting that the expansion of stem cells during the culture is associated with a higher success rate of transplantation. In addition, Matrigel-containing organoid suspensions transplanted better than organoids suspended in PBS (**Supplementary Fig. 5**; $P < 0.05$, Mann-Whitney U test), proposing a role for the simultaneous supply of extracellular matrix in successful transplantation.

Engraftment of organoids derived from a single Lgr5$^+$ cell

We next sought to initiate the protocol described above from a single stem cell (**Supplementary Fig. 6a**). We crossed *Lgr5-EGFP-ires-CreERT2* mice with *R26R-Confetti* reporter mice[30]. In the resulting offspring, tamoxifen-induced Cre activation resulted in Cre-mediated recombination at the *Rosa26* locus in individual Lgr5$^+$ stem cells, leading to stochastically selected expression of one out of four fluorescent proteins: red fluorescent protein (RFP), cyan fluorescent protein (CFP), GFP or yellow fluorescent protein (YFP). At 3 d after Cre activation, we sorted cells double positive for Lgr5-EGFP and Confetti-RFP, which consisted of ~0.02% of the total cells (**Fig. 5a**), equivalent to ~100 cells per mouse.

We cultured the sorted cells after a limiting dilution (100 cells per 96 well) using the Hubrecht protocol (Online Methods; protocol described previously[12] with addition of Y-27632 in the first 2 d). Four stem cells double positive for Lgr5-EGFP and Confetti-RFP grew out, which was comparable to the culture efficiency of small intestinal stem cells[11] (**Fig. 5b**). Organoids were expanded to more than 100 wells in >10 weeks, frozen and shipped. After thawing, we recovered the cells under the TMDU protocol. We transplanted ~500 organoids per recipient mouse, as described above. Analyses at 4, 17, 21 and 25 weeks after transplantation revealed the presence of grafts in these mice (**Fig. 5c** and **Supplementary Figs. 6b,c** and **7a**). At 25 weeks after transplantation, RFP$^+$ cells still generated a single-layered epithelium. We noted no sign of adenomatous or dysplastic change in any of the transplanted areas (**Fig. 5d**). Again, all differentiated cell types, as well as Ki67$^+$ proliferating cells, were present at normal ratios (**Fig. 5e** and **Supplementary Fig. 7b**).

DISCUSSION

Here we describe methodologies to isolate, culture and transplant Lgr5$^+$ colon stem cells. Our observations confirm that *Lgr5* marks genuine stem cells that retain their self-renewal and multilineage-differentiation properties even after prolonged culture. A major difference between small-intestinal and colon-culture conditions is in the latter's requirement for Wnt. Although Wnt factors can initiate Wnt signals on their own, R-spondins (such as Rspo1) can only augment preexisting Wnt signals[31]. Because Paneth cells produce Wnt3, they serve as the center of organization of the stem cell niche[19]. At the colon crypt bottoms, secretory cells are located between the Lgr5$^+$ stem cells that—like Paneth cells—express CD24 (ref. 19). However, these CD24$^+$ secretory cells do not produce a sufficient amount of Wnt proteins *in vitro* (data not shown). Therefore, colon organoids cannot grow from Rspo1 alone but, rather, also require exogenous Wnt.

This study provides proof of principle that cultured Lgr5$^+$ cells can be used for stem-cell therapy to repair damaged epithelium. Transplanted cells adhere to and cover superficially damaged tissue. Further, engrafted recipient mice had higher body weights than ungrafted controls, implying a beneficial role for the donor cells in DSS-induced acute colitis. Although further optimization is clearly needed, the current study implies that *in vitro* expansion and transplantation of gastrointestinal stem cells may be a promising option for patients with severe gastrointestinal epithelial injuries.

Lgr5$^+$ stem cells divide once every day *in vivo*[6], thus defying the Hayflick limit[32]. They appear similarly unrestricted in their proliferative capacity *in vitro*, while they retain their original tissue identity. It is of interest that the Lgr5 protein is now known to reside in the Wnt receptor complex to function as a receptor for Rspo1 (refs. 33,34), which is a crucial component of long-term organoid culture systems that we have developed. As the resulting organoids have now been proven to be transplantable, the Lgr5$^+$ stem cell isolation and expansion technology may provide a simple and safe avenue for the development of new regenerative and gene-therapy strategies.

METHODS

Methods and any associated references are available in the online version of the paper at http://www.nature.com/naturemedicine/.

Note: Supplementary information is available on the Nature Medicine website.

ACKNOWLEDGMENTS

We thank M. Okabe (Osaka University) for EGFP transgenic mice and Y. Kato, J. Inazawa, I. Sekiya (TMDU), H. Snippert and R. Vries (Hubrecht Institute) for technical assistance. This study was supported by Grant-in-Aid for Scientific Research from the Japanese Ministry of Education, Culture, Sports, Science and Technology, by the Health and Labour Sciences Research Grants for Research on Intractable Diseases from Ministry of Health, Labour and Welfare of Japan, and by a grant from the European Research Council and from the Dutch Cancer Foundation.

AUTHOR CONTRIBUTIONS

T. Nakamura, H.C. and M.W. designed the study. S.Y., T. Nakamura and T.S. performed experiments and analyzed data. T. Nakamura, T.S. and H.C. wrote the paper. Y.N., T. Nagaishi and K.T. assisted in transplantation experiments. T.M., X.Z. and K.T. gave support in gene analysis. R.O. helped with the immunohistochemistry. S.I. advised on the electron microscopy. H.C. and M.W. gave conceptual advice and supervised the project.

COMPETING FINANCIAL INTERESTS

The authors declare competing financial interests: details accompany the full-text HTML version of the paper at http://www.nature.com/naturemedicine/.

Published online at http://www.nature.com/naturemedicine/.
Reprints and permissions information is available online at http://www.nature.com/reprints/index.html.

1. Potten, C.S., Booth, C. & Pritchard, D.M. The intestinal epithelial stem cell: the mucosal governor. *Int. J. Exp. Pathol.* **78**, 219–243 (1997).
2. Bjerknes, M. & Cheng, H. Intestinal epithelial stem cells and progenitors. *Methods Enzymol.* **419**, 337–383 (2006).
3. Barker, N., van de Wetering, M. & Clevers, H. The intestinal stem cell. *Genes Dev.* **22**, 1856–1864 (2008).
4. Crosnier, C., Stamataki, D. & Lewis, J. Organizing cell renewal in the intestine: stem cells, signals and combinatorial control. *Nat. Rev. Genet.* **7**, 349–359 (2006).
5. Radtke, F. & Clevers, H. Self-renewal and cancer of the gut: two sides of a coin. *Science* **307**, 1904–1909 (2005).
6. Barker, N. *et al.* Identification of stem cells in small intestine and colon by marker gene *Lgr5*. *Nature* **449**, 1003–1007 (2007).
7. Barker, N. *et al.* Lgr5^{+ve} stem cells drive self-renewal in the stomach and build long-lived gastric units *in vitro*. *Cell Stem Cell* **6**, 25–36 (2010).
8. Sangiorgi, E. & Capecchi, M.R. *Bmi1* is expressed *in vivo* in intestinal stem cells. *Nat. Genet.* **40**, 915–920 (2008).
9. Avansino, J.R., Chen, D.C., Woolman, J.D., Hoagland, V.D. & Stelzner, M. Engraftment of mucosal stem cells into murine jejunum is dependent on optimal dose of cells. *J. Surg. Res.* **132**, 74–79 (2006).
10. Tait, I.S., Evans, G.S., Flint, N. & Campbell, F.C. Colonic mucosal replacement by syngeneic small intestinal stem cell transplantation. *Am. J. Surg.* **167**, 67–72 (1994).

© 2012 Nature America, Inc. All rights reserved.

11. Sato, T. *et al.* Single Lgr5 stem cells build crypt-villus structures *in vitro* without a mesenchymal niche. *Nature* **459**, 262–265 (2009).
12. Sato, T. *et al.* Long-term expansion of epithelial organoids from human colon, adenoma, adenocarcinoma, and Barrett's epithelium. *Gastroenterology* **141**, 1762–1772 (2011).
13. Booth, C., Patel, S., Bennion, G.R. & Potten, C.S. The isolation and culture of adult mouse colonic epithelium. *Epithelial Cell Biol.* **4**, 76–86 (1995).
14. Whitehead, R.H., Demmler, K., Rockman, S.P. & Watson, N.K. Clonogenic growth of epithelial cells from normal colonic mucosa from both mice and humans. *Gastroenterology* **117**, 858–865 (1999).
15. Kanayama, M. *et al.* Hepatocyte growth factor promotes colonic epithelial regeneration via Akt signaling. *Am. J. Physiol. Gastrointest. Liver Physiol.* **293**, G230–G239 (2007).
16. Tahara, Y. *et al.* Hepatocyte growth factor facilitates colonic mucosal repair in experimental ulcerative colitis in rats. *J. Pharmacol. Exp. Ther.* **307**, 146–151 (2003).
17. Kim, K.A. *et al.* Mitogenic influence of human R-spondin1 on the intestinal epithelium. *Science* **309**, 1256–1259 (2005).
18. Wei, Q. *et al.* R-spondin1 is a high affinity ligand for LRP6 and induces LRP6 phosphorylation and β-catenin signaling. *J. Biol. Chem.* **282**, 15903–15911 (2007).
19. Sato, T. *et al.* Paneth cells constitute the niche for Lgr5 stem cells in intestinal crypts. *Nature* **469**, 415–418 (2011).
20. Gerbe, F. *et al.* Distinct ATOH1 and Neurog3 requirements define tuft cells as a new secretory cell type in the intestinal epithelium. *J. Cell Biol.* **192**, 767–780 (2011).
21. Watanabe, K. *et al.* A ROCK inhibitor permits survival of dissociated human embryonic stem cells. *Nat. Biotechnol.* **25**, 681–686 (2007).
22. Haramis, A.P. *et al. De novo* crypt formation and juvenile polyposis on BMP inhibition in mouse intestine. *Science* **303**, 1684–1686 (2004).
23. Fre, S. *et al.* Notch signals control the fate of immature progenitor cells in the intestine. *Nature* **435**, 964–968 (2005).
24. van Es, J.H. *et al.* Notch/γ-secretase inhibition turns proliferative cells in intestinal crypts and adenomas into goblet cells. *Nature* **435**, 959–963 (2005).
25. van Es, J.H., de Geest, N., van de Born, M., Clevers, H. & Hassan, B.A. Intestinal stem cells lacking the Math1 tumour suppressor are refractory to Notch inhibitors. *Nat. Commun.* **1**, 18 (2010).
26. Wong, G.T. *et al.* Chronic treatment with the γ-secretase inhibitor LY-411,575 inhibits β-amyloid peptide production and alters lymphopoiesis and intestinal cell differentiation. *J. Biol. Chem.* **279**, 12876–12882 (2004).
27. Okamoto, R. *et al.* Requirement of Notch activation during regeneration of the intestinal epithelia. *Am. J. Physiol. Gastrointest. Liver Physiol.* **296**, G23–G35 (2009).
28. Wirtz, S., Neufert, C., Weigmann, B. & Neurath, M.F. Chemically induced mouse models of intestinal inflammation. *Nat. Protoc.* **2**, 541–546 (2007).
29. Okabe, M., Ikawa, M., Kominami, K., Nakanishi, T. & Nishimune, Y. 'Green mice' as a source of ubiquitous green cells. *FEBS Lett.* **407**, 313–319 (1997).
30. Snippert, H.J. *et al.* Intestinal crypt homeostasis results from neutral competition between symmetrically dividing Lgr5 stem cells. *Cell* **143**, 134–144 (2010).
31. Binnerts, M.E. *et al.* R-Spondin1 regulates Wnt signaling by inhibiting internalization of LRP6. *Proc. Natl. Acad. Sci. USA* **104**, 14700–14705 (2007).
32. Hayflick, L. & Moorhead, P.S. The serial cultivation of human diploid cell strains. *Exp. Cell Res.* **25**, 585–621 (1961).
33. de Lau, W. *et al.* Lgr5 homologues associate with Wnt receptors and mediate R-spondin signalling. *Nature* **476**, 293–297 (2011).
34. Carmon, K.S., Gong, X., Lin, Q., Thomas, A. & Liu, Q. R-spondins function as ligands of the orphan receptors LGR4 and LGR5 to regulate Wnt/β-catenin signaling. *Proc. Natl. Acad. Sci. USA* **108**, 11452–11457 (2011).

© 2012 Nature America, Inc. All rights reserved.

ONLINE METHODS

Mice. *Rag2*$^{-/-}$ mice were from Taconic Farms and Central Laboratories for Experimental Animals. *EGFP* transgenic mice[29], *Lgr5-EGFP-ires-CreERT2* mice[6] and *R26R-Confetti* mice[30] are described elsewhere. Male and female mice were randomly used for all experiments. All animal experiments were performed with the approval of the Institutional Animal Care and Use Committee of TMDU.

TMDU protocol for crypt isolation and three-dimensional culture. The colonic tissue was minced and digested. The crypts were further purified by mechanical disruption and density gradient centrifugation. A total of 2,000 crypts were suspended in 200 µl of the collagen type I solution (Nitta Gelatin Inc.) and placed in 48-well plates. After polymerization, 500 µl of Advanced DMEM/F12 containing BSA (Sigma), mouse EGF (mEGF) (PeproTech), mWnt3a, mRspo1, mHGF and mNoggin (all from R&D Systems) was added (TMDU medium). For passage, the gel was digested, and then the organoids were disaggregated with EDTA. The dissociated organoids were mixed in type I collagen solution and used for culture. A Rho kinase inhibitor, Y-27632, was added for the first 2 d after the cells were propagated. Where indicated, to induce goblet cell differentiation, organoids were treated with LY-411575, a GSI. See details in the **Supplementary Methods**.

Chromosome analysis. Chromosome karyotyping was performed according to a standard protocol as detailed in the **Supplementary Methods**.

Stereomicroscopy, phase-contrast imaging and histology. Images were acquired on either a fluorescence microscope equipped with phase-contrast setting (BZ-8000, KEYENCE), a fluorescent stereomicroscope system MVX10 (Olympus) or a fluorescence microscope DeltaVision system (Applied Precision). For histology and immunohistochemistry, tissues and organoids were fixed, sequentially dehydrated in sucrose in PBS, and frozen in OCT compound (Tissue Tek). Cryosections were examined by conventional H&E, alcian blue staining and a spectrum of immunohistochemical reactions, as detailed in the **Supplementary Methods**.

Transmission electron microscopy. Transmission electron microscopy was performed in a standard fashion and is detailed in the **Supplementary Methods**.

Live imaging. Live imaging was performed on the DeltaVision system. A culture dish placed on the microscope stage was covered with a chamber in which a humidified premixed gas consisting of 5% CO_2 and 95% air was infused, and the whole setup was set at 37 °C. DIC and fluorescent images were acquired at 20-min intervals. The data were processed using Softworx (Applied Precision) and, if necessary, image editing was performed using Adobe Photoshop Elements 7.0.

Semi-quantitative RT-PCR. Semi-quantitative RT-PCR was performed in standard fashion. The primer sequences used are listed in **Supplementary Table 1**. PCR products were separated on agarose gels and visualized using ImageQuant TL system (GE Healthcare).

Sorting and Hubrecht-protocol culture for single Lgr5$^+$ cells. Tamoxifen was injected into *R26R-Confetti* mice crossed with *Lgr5-EGFP-ires-CreERT2* mice, and the colonic crypts from the resulting mice were isolated 3 d later. Epithelial cells were dissociated with TrypLE express (Invitrogen) and analyzed by MoFlo (DakoCytomation). Viable single cells were gated, and then the cells doubly positive for EGFP and RFP were sorted and embedded in Matrigel (BD Bioscience) on 96-well plates. An Advanced DMEM/F12 culture medium supplemented with penicillin and streptomycin, 4-(2-hydroxyethyl)-1-piperazineethanesulfonic acid (HEPES), glutamax, N2, B27 (all from Invitrogen) and growth factors (EGF, noggin and R-spondin) was diluted 1:1 with Wnt3a-conditioned medium and used as Hubrecht medium. Y-27632 was included for the first 2 d to avoid anoikis. Growth factors were added every other day, and the entire medium was changed every 4 d. See the **Supplementary Methods** for additional details.

Transplantation experiments. For the EGFP$^+$ cell transplantations, cells isolated from colon tissues were cultured for 5 or 8 d according to the TMDU protocol and used as donor cells. For single Lgr5$^+$-cell–derived organoid transplantation, cells were expanded based on the Hubrecht protocol and then cryopreserved. The cells were then shipped, thawed and further cultured. Acute colitis was induced by feeding 6-week-old *Rag2*$^{-/-}$ mice with 3.0% DSS (molecular weight 10,000; Ensuiko Sugar Refining Co.) dissolved in drinking water for 5 d (days 1–5). At 7 and 10 d after the start of DSS administration, donor cells equivalent to those from ~500 organoids were instilled into colonic lumen as a suspension. After infusion, the anal verge was glued for 6 h. After the transplantation on day 10, mice were maintained as usual before they were killed and analyzed. See the **Supplementary Methods** for additional details.

TRITC-dextran permeability assay. Intestinal permeability was assessed by enteral administration of TRITC-dextran (molecular mass 4.4 kDa; Sigma). Transplanted or sham-transplanted mice were gavaged with TRITC-dextran 4 h before killing on day 38. Whole blood was obtained at the time of killing, and then the colonic tissues were examined for whether the EGFP$^+$ engrafts were present. TRITC-dextran measurements were performed on an ARVO MX (PerkinElmer), with serial dilutions of TRITC-dextran used as a standard curve.

Statistical analyses. Data are shown as means ± s.e.m. Data for **Figures 3f**, **4d** and **Supplementary Figure 7b** were statistically analyzed by the two-sample Student's *t* test. The data for **Supplementary Figure 5** showed non-normal distributions and were analyzed by Mann-Whitney *U* test. Statistical significance for comparisons was assigned at $P < 0.05$.

Additional methods. Detailed methodology is described in the **Supplementary Methods**.

© 2012 Nature America, Inc. All rights reserved.

doi:10.1038/nm.2695

Reproduced with permission of the copyright owner. Further reproduction prohibited without permission.

Please cite this article in press as: Fordham et al., Transplantation of Expanded Fetal Intestinal Progenitors Contributes to Colon Regeneration after Injury, Cell Stem Cell (2013), http://dx.doi.org/10.1016/j.stem.2013.09.015

Cell Stem Cell
Article

Transplantation of Expanded Fetal Intestinal Progenitors Contributes to Colon Regeneration after Injury

Robert P. Fordham,[1,2,6] Shiro Yui,[3,4,6] Nicholas R.F. Hannan,[1,2] Christoffer Soendergaard,[5] Alison Madgwick,[1] Pawel J. Schweiger,[3] Ole H. Nielsen,[5] Ludovic Vallier,[1,2] Roger A. Pedersen,[1,2] Tetsuya Nakamura,[4] Mamoru Watanabe,[4] and Kim B. Jensen[1,3,*]

[1]Wellcome Trust & Medical Research Council Cambridge Stem Cell Institute, Cambridge, CB2 1QR, UK
[2]Anne McLaren Laboratory for Regenerative Medicine, Department of Surgery, University of Cambridge, Cambridge, CB2 0SZ, UK
[3]BRIC: Biotech Research and Innovation Centre, University of Copenhagen, DK-2200 Copenhagen N, Denmark
[4]Department of Gastroenterology and Hepatology, Tokyo Medical and Dental University, Bunkyo-ku, Tokyo, 113-8519, Japan
[5]Department of Gastroenterology, Medical Section, Herlev Hospital, Faculty of Health and Medical Sciences, University of Copenhagen, DK-2730 Herlev, Denmark
[6]These authors contributed equally to this work
*Correspondence: kim.jensen@bric.ku.dk
http://dx.doi.org/10.1016/j.stem.2013.09.015
This is an open-access article distributed under the terms of the Creative Commons Attribution License, which permits unrestricted use, distribution, and reproduction in any medium, provided the original author and source are credited.

SUMMARY

Regeneration and homeostasis in the adult intestinal epithelium is driven by proliferative resident stem cells, whose functional properties during organismal development are largely unknown. Here, we show that human and mouse fetal intestine contains proliferative, immature progenitors, which can be expanded in vitro as Fetal Enterospheres (FEnS). A highly similar progenitor population can be established during intestinal differentiation of human induced pluripotent stem cells. Established cultures of mouse fetal intestinal progenitors express lower levels of Lgr5 than mature progenitors and propagate in the presence of the Wnt antagonist Dkk1, and new cultures can be induced to form mature intestinal organoids by exposure to Wnt3a. Following transplantation in a colonic injury model, FEnS contribute to regeneration of colonic epithelium by forming epithelial crypt-like structures expressing region-specific differentiation markers. This work provides insight into mechanisms underlying development of the mammalian intestine and points to future opportunities for patient-specific regeneration of the digestive tract.

INTRODUCTION

Fertilization of the oocyte initiates a series of events that, following gastrulation, leads to organ formation in the developing fetus. During this process, pluripotent stem cells progressively lose potential as the early embryo is patterned along its axes and organ structures are specified. Tissue-specific programs subsequently direct the formation and maturation of adult organs, which are maintained throughout life by stem cells with tissue-restricted lineage potential. It remains unclear whether transitory stem cell states exist in the embryo, responsible for tissue maturation, or whether maturation is achieved via adult tissue-specific stem cells in the fetal tissue. Understanding the process of tissue maturation in vivo has implications for the directed differentiation of pluripotent cells into functionally mature tissue types (Zorn and Wells, 2009).

The intestinal epithelium is continuously replenished by resident stem cells. The mature mammalian small intestine is a tube-like structure with an inner epithelial lining facing the lumen. This layer is organized into differentiated villi protruding into the lumen and proliferative crypt compartments invaginated into the underlying mesenchyme. Intestinal Stem Cells (ISCs) reside at the crypt base and give rise to all the differentiated cell types (Barker et al., 2007, 2012). Development of the small intestine follows a specific pattern. Villus formation in humans begins around the ninth week of gestation and embryonic day 15 (E15) in mouse. In the human, crypt formation occurs before birth, whereas in the mouse this happens during the first 2 postnatal weeks (Montgomery et al., 1999; Spence et al., 2011a). Beyond these morphological rearrangements, the mechanisms of initial intestinal lineage differentiation and functional maturation are less well characterized. Despite temporal differences in the ontogeny of the small intestine between human and mouse, the overall process of development is identical, making the mouse an accessible model to interrogate the process of human intestinal maturation.

Our understanding of the mature intestine has been accelerated by the establishment of culture conditions for long-term maintenance of adult mouse and human intestinal epithelium in vitro (Jung et al., 2011; Sato et al., 2009, 2011a). In this system, single ISCs or dissociated crypt fragments are embedded in Matrigel where they exhibit self-organization into "mini-guts." Here we describe the identification of proliferative progenitors captured in the human fetal intestine and during intestinal differentiation of human induced pluripotent stem cells (hiPSCs). This

Please cite this article in press as: Fordham et al., Transplantation of Expanded Fetal Intestinal Progenitors Contributes to Colon Regeneration after Injury, Cell Stem Cell (2013), http://dx.doi.org/10.1016/j.stem.2013.09.015

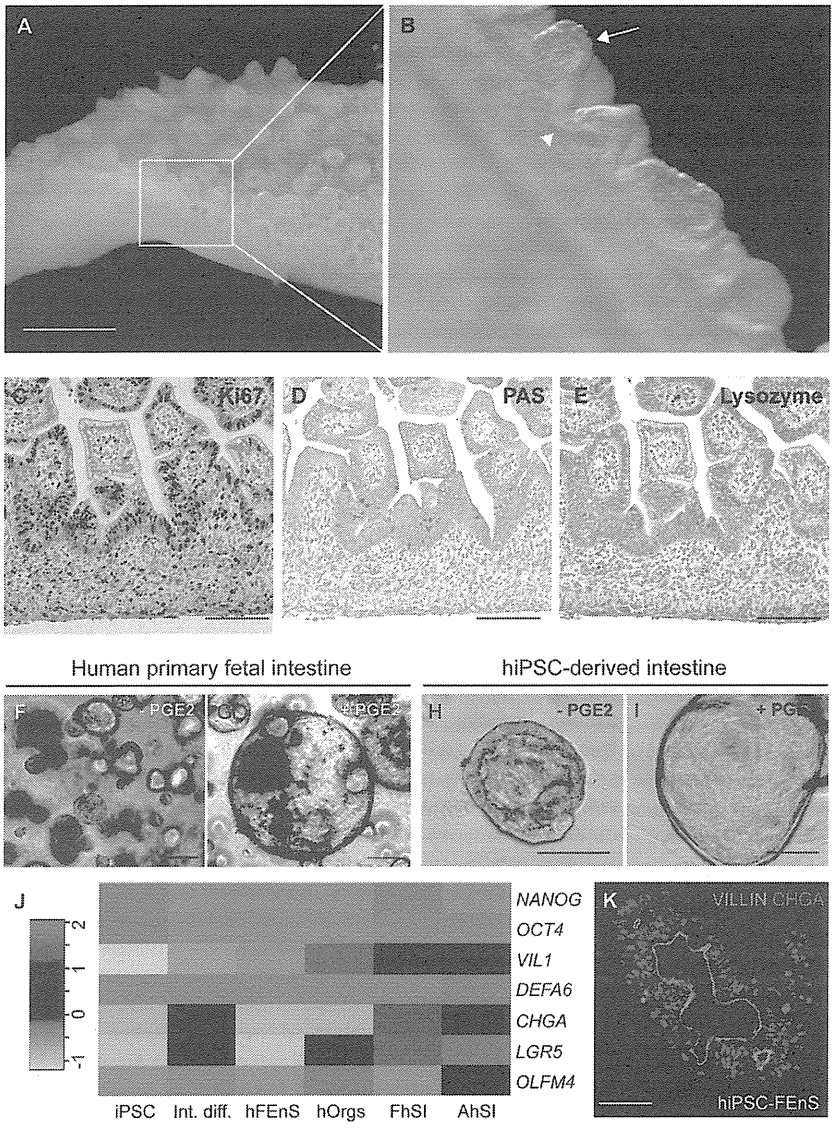

Figure 1. Derivation of Immature Intestinal Progenitors from Human Fetal and Pluripotent Cells

(A) Whole mount of human gestational week 10 small intestine.

(B) Higher magnification of villi (arrow) and intervillus regions (arrowhead) in (A).

(C–E) Immunohistochemistry analysis for Ki67 (C), PAS staining (D), and Lysozyme (E) in week 10 human small intestine.

(F and G) Spheroid cultures from week 10 human small intestinal epithelium, grown with (G) and without (F) prostaglandin E2 (PGE2) (2.5 μM).

(H and I) Intestinal tissue derived from directed differentiation of human induced pluripotent stem cells (hiPSCs), cultured with (I) and without (H) PGE2.

(J) Relative expression levels of intestinal lineage markers in material from undifferentiated human induced pluripotent stem cells (hiPSC), iPSC-derived intestine (Int. diff.), human primary fetal enterospheres (hFEnS), human adult organoids (hOrgs), primary fetal human small intestine (FhSI), and primary adult human small intestine (AhSI). Red and green colors reflect increased and decreased deviation from the mean, respectively.

(K) Detection of VILLIN (green) and CHGA (red) in hiPSC-FEnS.

The scale bars represent 2 mm in (A) and 100 μm in (C)–(E) and (K). See also Figure S1 and Table S1.

is recapitulated in murine tissues, where fetal progenitors can transition spontaneously and by Wnt induction into an adult state. Finally, we present evidence that fetal progenitors can contribute to the regeneration of adult colonic epithelium in vivo, as proof of principle that developmentally immature cells have clinical potential.

RESULTS

Fetal Human Intestinal Epithelium Can Be Propagated Long-Term In Vitro as Fetal Enterospheres

Previous studies have described the establishment of organoid cultures from mature human gut epithelium (Jung et al., 2011; Sato et al., 2011a). To investigate the in vitro potential of immature gut epithelium, we analyzed human fetal intestinal tissue around gestational week 10. At this stage, crypts have not formed and the human intestine consists of a series of undulating villi, with proliferation localized primarily to the intervillus regions (Figures 1A–1C). Here a subset of cells is weakly positive for Periodic Acid Schiff's (PAS), though they do not have the mature morphology of goblet cells and there are no detectable Lysozyme^{+ve} Paneth cells (Figures 1D and 1E). The reduced level of secretory differentiation was confirmed at the transcriptional level (Figure 1J).

Fetal human intestinal tissue at around gestational week 10 was dissected and dissociated epithelial fragments were seeded in Matrigel. The conditions used for propagation of adult murine organoids (EGF, Noggin, and R-spondin1 [ENR]) caused the growth of small granular spheres that could not be maintained long-term without the addition of prostaglandin-E2 (PGE2) (Figures 1F and 1G). We term these human Fetal Enterospheres (hFEnS). hFEnS are highly proliferative and can be passaged repeatedly by mechanical dissociation for over 2 months with no spontaneous transition into budding organoids during this time.

Intestinal Tissue from Human Pluripotent Cells Has Fetal Characteristics

Human induced pluripotent stem cells (hiPSCs) can be differentiated into intestinal epithelium (Spence et al., 2011b). We set out to determine whether hiPSC-derived intestinal tissue transitions through a fetal state. Using a chemically defined protocol, PSCs were directed toward definitive endoderm (DE) and further

patterned into posterior DE (Hannan et al., 2013). Raised aggregates of cells forming from the sheet of posteriorized endoderm were transferred as small clumps to Matrigel (Figure S1A available online). Again PGE2 facilitated the formation of larger cystic epithelial spheroids, morphologically analogous to primary hiFEnS (Figures 1H and 1I). These structures were maintained for over 2 months, through repeated passaging. In both cases PGE2 provides a pro-proliferative signal that drives the growth of spherical structures. hiPSC-FEnS also require low levels of Wnt3a to support growth, suggesting that although morphologically alike, they possess slightly different properties. Expression analysis verifies the immature nature of human FEnS and hiPSC-FEnS when compared to human adult organoids as well as fetal and adult intestine (Figures 1J and S1B). iPSC-derived FEnS had Villin present at the apical cell membrane in the spherical structure, and its immature nature is further supported by the lack of secretory Chromogranin-A^{+ve} cells (Figure 1K).

Establishment of FEnS from Immature Mouse Intestine

We reasoned that development of the mouse intestine would provide an accessible model system to interrogate intestinal maturation more closely. The mouse intestine at embryonic day 16 (E16) resembles the human intestine at around 10 gestational weeks with high proliferation in the intervillus regions and scattered immature goblet cells (Figures 2A, S2A, S2B, S2E, and S2F). By postnatal week 2, mature crypts are forming (Figures 2B, S2C, and S2D) and mature Lysozyme^{+ve} Paneth cells can now be detected in the proliferative zones (Figures S2G and S2H). The appearance of secretory cells is also evident by expression analysis during the course of intestinal development (Figure 2C).

To investigate whether fetal murine intestine contains equivalent FEnS progenitors, we seeded epithelial cells from the proximal half of the small intestine. During a developmental time course, we observed that FEnS form exclusively up to P2, whereas organoids are formed from P15 and onward (Figures 2D–2F and 2I). Interestingly, analysis of material from P2 to P15 illustrates the formation of both FEnS and organoids with an increasing fraction of the latter (Figures 2G–2I). Murine FEnS (mFEnS) are morphologically indistinguishable from hFEnS and can be expanded through fortnightly passaging for at least 2 years (Passage n $\approx$ 100). During their serial passaging we observe no spontaneous maturation or morphological and karyotypic alterations (Figure 2J). Although PGE2 is not required for maintenance of mFEnS, it does provide a pro-proliferative effect independent of Wnt signaling (Figure S2I). As has been reported for the adult colonic cultures, this is most likely via cAMP-mediated block of anoikis and stimulation of MAP kinase signaling (Jung et al., 2011). Established mFEnS can grow without R-spondin1 and in the presence of the natural Wnt antagonist DKK1, Porcupine inhibitor (which inhibits Wnt secretion), and tankyrase inhibitor (which stabilizes the Axin2/APC complex responsible for degradation of β-catenin), hereby demonstrating that FEnS can be maintained independently of Wnt signaling (Figures S2J and S2K). This distinguishes them from adult organoids.

Characterization of mFEnS revealed that they consist of a polarized epithelium with Villin localized to the apical surface, similar to the small intestine (Figures 2K and 2L). Moreover, FEnS phenocopy the differentiation patterns of the immature epithelium as there are no detectable secretory cell markers at both the protein and RNA level and reduced expression of adult stem cell markers (Figures 2M–2P and S3A). BrdU incorporation analysis showed that proliferative cells in mFEnS are scattered across the whole surface, whereas proliferative zones in organoids are restricted to the crypt domains (Figures 2Q and 2R). The overall morphology and growth of FEnS as spheres are reminiscent of that reported for organoids that form as a result of augmented Wnt signaling following loss of APC (Sato et al., 2011b). However, expression analysis demonstrates distinct expression patterns between FEnS and APCnull organoids (Figure S3B). In particular, it is clear that loss of APC causes increased levels of adult stem cell markers, whereas these are generally reduced in the fetal state (Figure S3B). In summary, this demonstrates that progenitors within the fetal small intestine have a unique behavior that sets them aside from both normal and cancerous adult stem cells.

In Vitro Maturation of Fetal Enteric Progenitors

Intestinal maturation in vivo has been proposed to follow a wave from proximal to distal sites (Spence et al., 2011a). To assess the positional effect along the length of the small intestine, we analyzed the regional differences in in vitro growth potential at postnatal day 2 (Figure 3A). Contrary to expectations, FEnS formed from proximal tissue, whereas more distal tissues formed organoids (Figures 3A and 3B). Gene expression analysis showed that the ability to form organoids correlates with increased levels of *Lgr5* and *Axin2* (Figure 3C). Analysis of the cultured material from the proximal and mid regions of the small intestine shows variable but comparable expression of Wnt target genes, suggesting that FEnS can respond to Wnt stimulation and that this represents a transitory and dynamic cellular state (Figure 3D). In line with the observed adult stem cell behavior, the distal part of the small intestine expresses higher levels of secretory lineage markers, which are characteristic of the adult small intestine, and contains a greater number of *Ulex europaeus* agglutinin I (UEA-I) reactive secretory cells (Figures 3C, 3E–3E″, and 3F). This further supports a distal to proximal wave of tissue maturation.

In the mature intestine, Lgr5 marks ISCs, and single sorted Lgr5^{+ve} cells give rise to adult organoids (Barker et al., 2007; Sato et al., 2009). In the immature intestine Lgr5 is expressed by cells in the intervillus regions (Figure 4A). We hypothesized that Lgr5 expression defines progenitors permissive for transitioning into the adult state. In line with this, Lgr5-GFP^{+ve} cells sorted from neonatal intestinal epithelium form organoids in vitro, whereas FEnS are formed from cells in the Lgr5-GFP^{-ve} population (Figures 4B–4E). It is impossible to assess whether organoids form exclusively from Lgr5^{+ve} cells, as a large proportion of Lgr5-expressing cells in the Lgr5 knockin model are EGFP^{-ve} due to the mosaic nature of the mouse model.

To assess the relationship between organoids and FEnS, we analyzed samples from P2. Approximately one-half of the structures grow in a manner indistinguishable from fetal tissues (Figure S4A, Movie S1), whereas the rest followed a distinct pattern indicative of spontaneous differentiation (Figure S4B, Movie S2). All structures grow exponentially for around 7 days. At this point some structures collapse and start to form budding

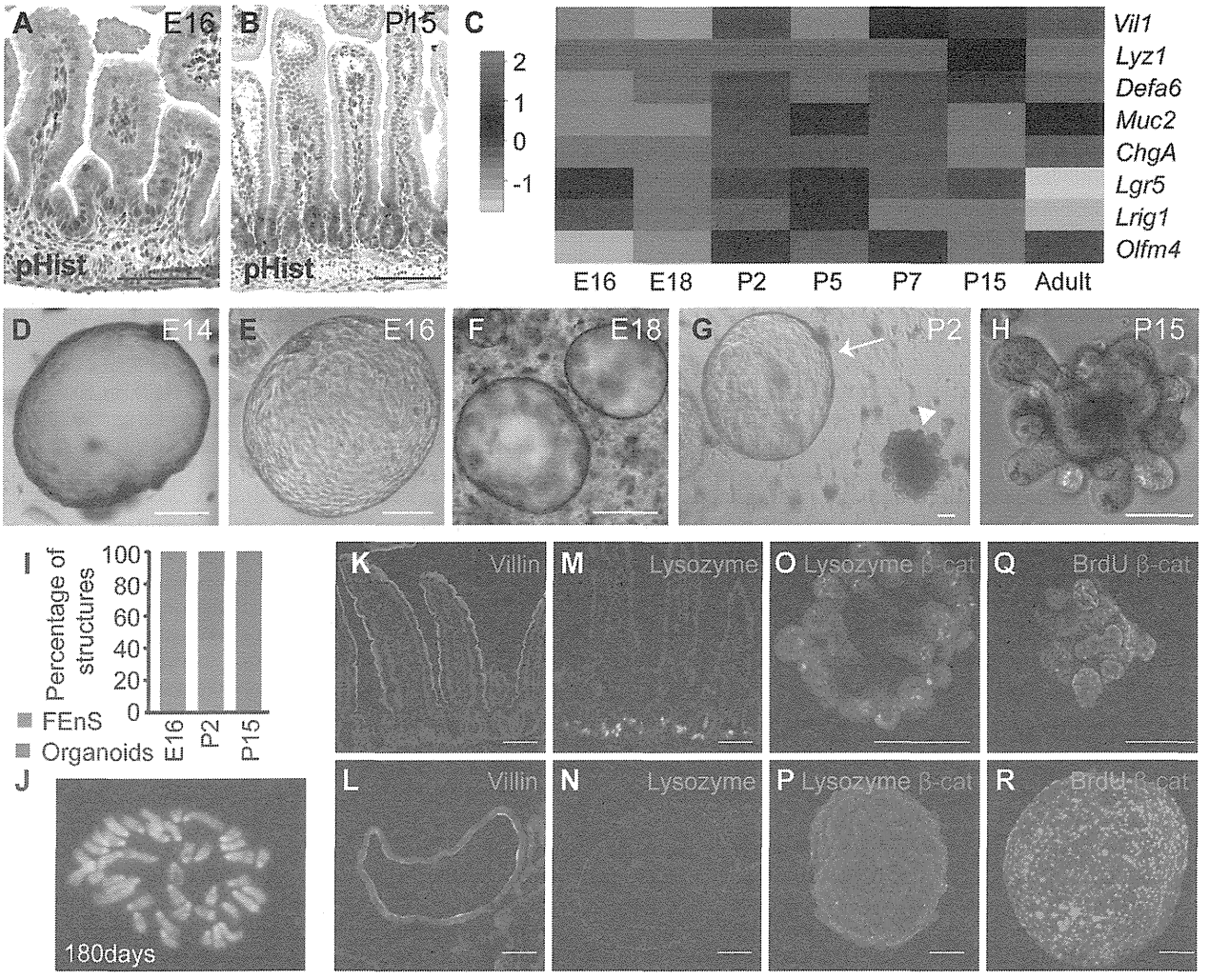

Figure 2. Establishment of mFEnS from Immature Mouse Intestine

(A and B) Immunohistochemistry analysis for Phospho-Histone-H3 (pHist) on sections of small intestine from E16 mice (A) and P15 mice (B).

(C) Relative expression levels of intestinal lineage markers in tissue isolated from proximal murine intestine at increasing developmental age from E16 to adult. Red and green colors reflect increased and decreased deviation from the mean, respectively.

(D–H) Representative images of in vitro structures derived from E14 to P15. The arrow and arrowhead in (G) indicate an FEnS and an organoid, respectively.

(I) Relative proportions of FEnS and organoids present after 2 weeks from E16, P2, and P15 tissues.

(J) Metaphase spread of a cell at day 180 shows a normal karyotype (n = 15).

(K and L) Detection of apical villin expression (green) in adult small intestine (K) and mFEnS (L).

(M–P) Lysozyme expression in adult small intestine (M), cross sections of mFEnS (N), and whole-mount organoids and mFEnS (O and P).

(Q and R) BrdU incorporation analysis in whole mounts of organoids and FEnS (green). β-catenin (red) is used as a counterstain.

The scale bars represent 100 μm. E, embryonic day; P, postnatal day; adult, >3 weeks postnatal. See also Figures S2 and S3.

protrusions from the surface (Figure S4B). After passaging, these P2 organoids become R-spondin1 dependent and identical to structures obtained from more mature intestinal tissue (Figure S4C, Movie S3).

Since *Lgr5* and *Axin2* are both Wnt target genes, and given the dynamic regional expression correlating with organoid formation (Figure 3D), we investigated whether Wnt3a can induce intestinal maturation in vitro. Stimulation of cells from E16 proximal intestine, which normally only form FEnS, promoted the transition into budding organoids in a proportion of the forming structures (Figure S4D). This effect is enhanced upon passaging and the forming organoids can subsequently be maintained without exogenous Wnt in an R-spondin1-dependent manner (Figure S4Dix). Continued culture of organoids with high levels of exogenous Wnt3a produced the cystic morphology previously described for Wnt overactivity in adult cultures (Sato et al., 2011b; Figures S4vi and S4vii). In contrast, FEnS could not be induced to transit to an adult state with Wnt3a (Figures S4iv and S4v). The observed Wnt-stimulated maturation of FEnS to organoids is associated with the expected upregulation of secretory lineage markers (Figure S4E). It is clear that FEnS respond to Wnt stimulation, as *Lgr5* and *Axin2* expression is elevated compared to

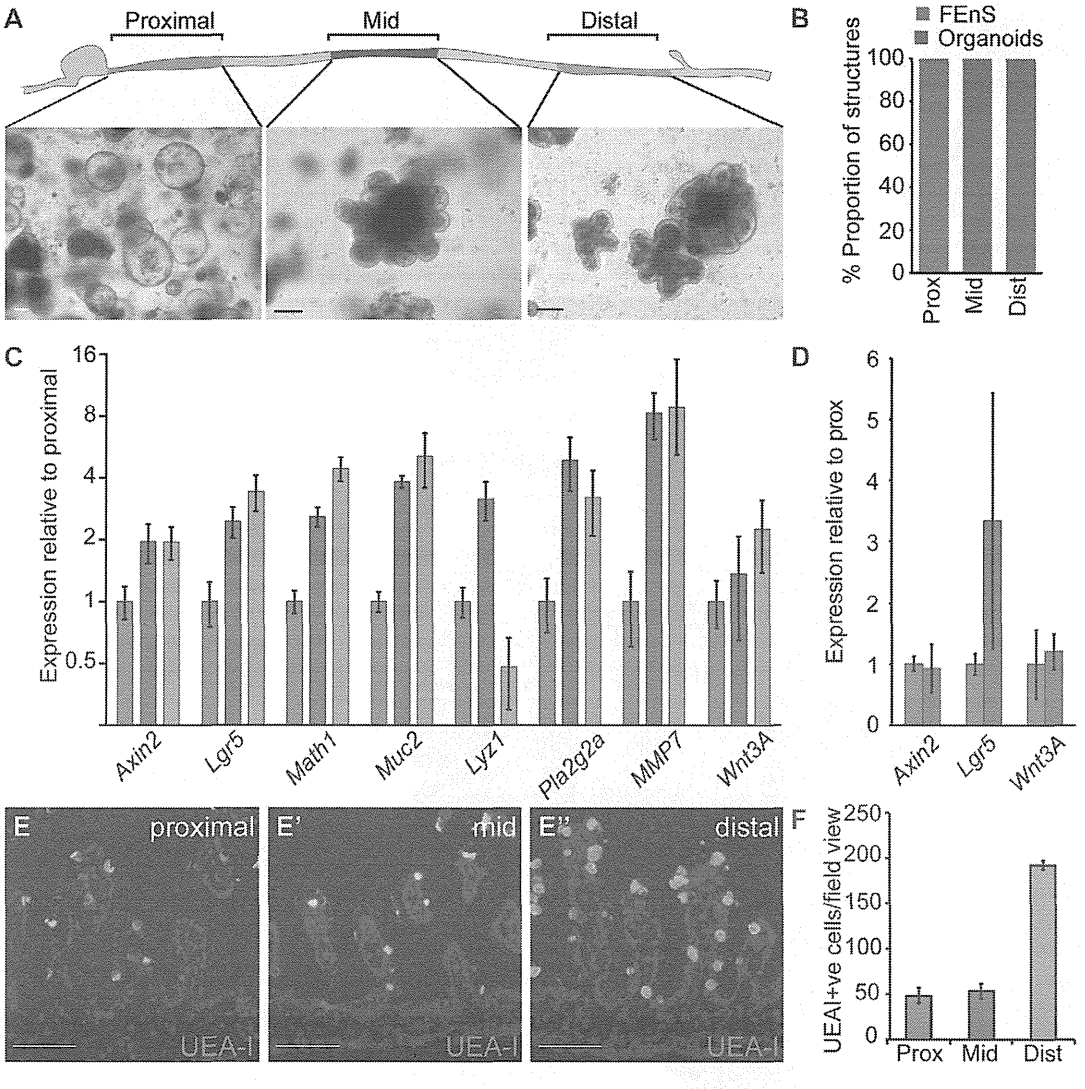

Figure 3. Adult Stem Cell Behavior Follows a Caudal to Rostral Pattern

(A) Schematic diagram of the Proximal, Mid, and Distal parts of the small intestine and the representative images of cultures derived at P2.

(B) Relative proportion of FEnS and organoids in the different sections of the small intestine.

(C) Expression analysis in material isolated from Proximal, Mid, and Distal regions. Data represent the mean, and the error bars, the SEM (n = 3). Data are expressed relative to Proximal, on a Log_2 scale.

(D) Expression analysis of cultures from proximal and mid intestine enriched for FEnS and organoids, respectively. Data represent the mean, and the error bars, the SEM (n = 3), and are normalized to proximal cultures.

(E) Detection of cells of the secretory lineage based on binding of *Ulex europaeus* agglutinin I (UEA-I) in the proximal, mid, and distal small intestine.

(F) Quantification of UEA-I^{+ve} cells. Data represent the mean, and the error bars, the SEM (n = 3).

The scale bars represent 100 μm.

established cultures and also newly transitory organoids (Figure S4E); however, the signal is insufficient to induce maturation.

In order to further probe the functional significance of Wnt in the transition from a fetal to an adult phenotype, epithelial cells were isolated from P2 proximal small intestine. Because a proportion of FEnS at this stage naturally transition to the adult organoids, it is possible to investigate the importance of Wnt signaling in the establishment of both organoids and FEnS, as well as the transition between the two states. Epithelial cells were isolated from the Lgr5-reporter model in order to visualize Lgr5 expression. Whenever we observe high Lgr5-EGFP expression, this is in association with structures that are beginning to transition into the adult state. In medium supplemented with ENR, $EGFP^{+ve}$ cells can be found either in mature crypt domains (Figures 4F and 4F′) or in regions with columnar morphology (Figures 4G and 4G′), whereas FEnS structures are seemingly $EGFP^{-}$ve or dim (Figures 4H and 4H′). The addition of Wnt increases the number of formed organoids (Figure 4N) and the regions of Lgr5 expression in the developing structures. This varies from single positive buds to extensive regions of Lgr5-$EGFP^{+ve}$

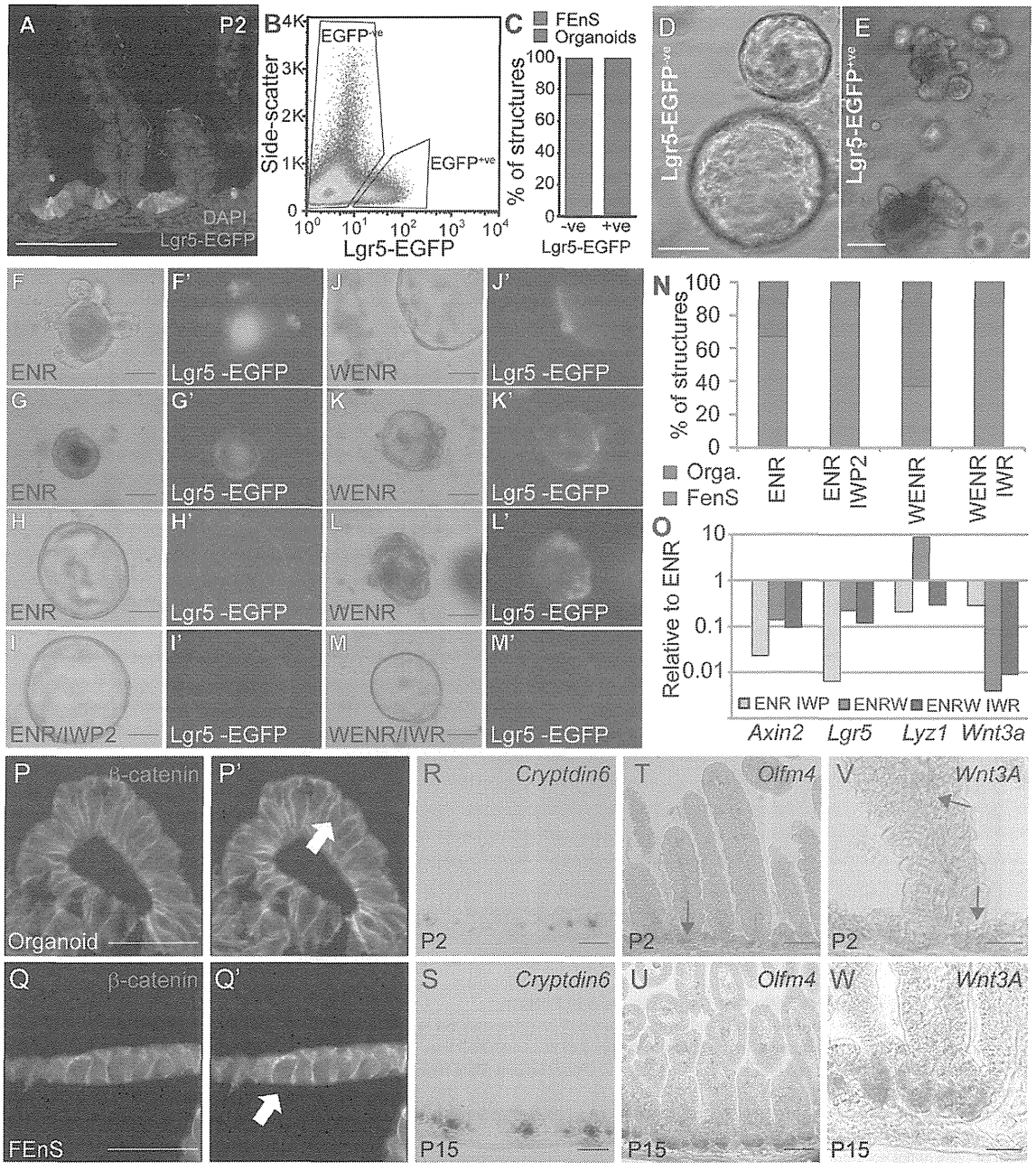

Figure 4. In Vitro Maturation of Fetal Enteric Progenitors Is Associated with Lgr5 Expression and Wnt Signaling

(A) Detection of Lgr5-EGFP at P2 from Lgr5-EGFP-ires-CreERT2 mice.

(B) Isolation of Lgr5-GFP^{+ve} and Lgr5-GFP^{-ve} epithelial cells from P2 small intestine by flow cytometry.

(C) Quantification of proportion of FEnS and organoids formed in vitro from Lgr5-GFP^{-ve} and Lgr5-GFP^{+ve} neonatal intestinal epithelial cells.

(D and E) Representative images of structures formed in vitro from Lgr5-GFP^{-ve} and Lgr5-GFP^{+ve} neonatal intestinal epithelial cells.

(F–M) Representative images of FEnS and organoids derived from Lgr5-EGFP-ires-CreERT2 mice and cultured in the presence of EGF, Noggin, and R-spondin1 (ENR), ENR and the porcupine inhibitor IWP2 (ENR/IWP2), ENR and Wnt3a (WENR), or WENR in the presence of the tankyrase inhibitor IWR (WENR/IWR). (F′)–(M′) show grayscale images of EGFP in the derived structures.

(N) Quantification of proportion of FEnS and organoids formed in the different treatment groups (ENR: 18/8; ENR/IWP2: 26/0; WENR: 21/30; WENR/IWR: 33/0). Two-tailed Fisher's exact test shows significant difference between ENR and ENR/IWP2 ($p = 0.0042$), ENR and WENR ($p = 0.0297$), and WENR and WENR/IWR ($p < 0.0001$).

(O) Expression analysis of the different treatment groups normalized to the ENR condition. Data represent the mean ($n = 2$).

(P and Q) Detection of β-catenin (green) in organoids and FEnS. Arrows indicate cells with nuclear localization of β-catenin suggestive of active signaling.

(legend continued on next page)